Full-potential linear-muffin-tin-orbital method for calculating total energies and forces

S. Yu. Savrasov*
Max-Planck-Institut für Festkörperforschung, 7000-Stuttgart 80, Federal Republic of Germany

D. Yu. Savrasov
P. N. Lebedev Physical Institute, Leninskii Prospect 53, Moscow, Russia
(Received 13 July 1992)

We present an efficient scheme for including full-potential terms in the linear-muffin-tin-orbital method. It is based on direct evaluation of the integrals in the intersitial region by partitioning crystalline space into atomic-cell envelopes and using one-center spherical harmonics expansions. This leads to a fast and accurate method for *ab initio* total-energy frozen-phonon calculations. The formulation for atomic forces is also given in this framework. Test results for phonon frequencies in a semiconductor, a transition metal, and a simple metal obtained from both the total-energy and force calculations are presented and found to be in good agreement with experiments.

I. INTRODUCTION

During the last decade a number of methods have been elaborated for performing self-consistent total-energy calculations which do not use any shape approximation of either potential or charge density inside the elementary cell. Based on density-functional theory (DFT) in its local-density approximation[1] (LDA) these full-potential methods have made it possible to compute from first principles a great number of physical properties such as, for example, lattice dynamical properties,[2] static response functions,[3] and relaxation effects around impurities.[4] One of the basic applications is the prediction of equilibrium structure and phonon frequencies of a solid. Usually, this is done in terms of the frozen-phonon approach,[5] i.e., by calculating the total energy or the atomic forces for different positions of the atoms and then obtaining the dynamical matrix by fitting the total-energy (force) versus the displacements. The energies or forces are only sufficiently accurate if all the nonspherical terms in the potential (so-called non-muffin-tin corrections) are taken into account properly.

The standard technique for solving the Schrödinger equation with a potential of arbitrary shape is to use the variational principle. The important question which arises in this connection is the construction of appropriate trial functions representing a Bloch state of a valence electron. Usually, space is partitioned into nonoverlapping muffin-tin (MT) spheres centered on each atom and the remaining interstitial region. Within the spheres the basis functions are represented in terms of numerical solutions of the radial Schrödinger equation for the spherical part of the potential multiplied by spherical harmonics. In the interstitial region where the potential is essentially flat they are taken from the solutions of Helmholtz's equation: $(-\nabla^2-\varepsilon)f(\mathbf{r})=0$. In the popular LAPW (linear augmented plane-wave) method[6,8] the basis functions are plane waves which are joined smoothly to spherical Schrödinger-equation solutions at the sphere boundaries. While this complete set can, in principle, reproduce the correct behavior of Bloch states in the interstitial region the slow convergence of plane waves in the case of materials with open structures or supercells imposes severe restrictions on the speed of the method.

The localized orbital representation and, especially, the representation of linear-muffin-tin orbitals (LMTO's),[7] on the other hand, is well known for its fast basis convergence. The LMTO's in the interstitial region are the linear combinations of Bessel and Hankel functions which are taken with some fixed energy $\varepsilon=\kappa^2$. In particular, in the LMTO method[6] using atomic-sphere approximation (ASA) with $\kappa^2=0$, only nine orbitals per atom are typically needed to reproduce energy bands with an accuracy better than 1 mRy. Much effort has been made to account for non-MT corrections carefully in this framework. Weyrich suggested the use of a Fourier transformation for LMTO's in the interstitial region.[9] This does not increase the size of the Hamiltonian and overlap matrices but makes the construction of charge density a tedious problem. The direct calculation of the charge density via the real space tight-binding representation was used by Blöchl.[10] A technique for handling with full density in all space has been recently proposed by Methfessel.[11,16] Using the values and gradients at the spheres the product of two LMTO's is fitted by linear combination of two Hankel functions and thus the density can be found by an extrapolational procedure.

In this paper we shall use the angular momentum representation for all the relevant quantities within MT spheres as well as in the interstitial region. We partition the crystalline space into atom-centered polyhedral cell envelopes and expand LMTO's in spherical harmonics inside spheres surrounding them. These one-center expansions will correctly define the charge density only within polyhedra. Consequently, the problems of solving Poisson's equation and evaluating matrix elements of the full potential are reduced to finding an efficient way of integrating the function over the region between the MT sphere and polyhedron boundary. The latter can be car-

ried out either by applying the θ-function-expansion technique[7] or, as we show below, by reducing the volume integrals to surface ones in terms of the Gauss theorem. The advantage of the present approach is that only the spherical harmonics representation is used, which leads to a method whose computational speed is only a few times slower compared with the LMTO-ASA calculations. It keeps the physical transparency of the standard LMTO method and can be inserted rapidly into existing programs. Below, a specific implementation for the problem of lattice dynamics is considered. An all-electron formulation for atomic forces is given which represents the force as a Hellman-Feynman contribution plus the so-called incomplete-basis set correction (Pulay force).[12] The method is applied for calculating optical Γ phonons in Si, boundary H phonons in Nb, and X phonons in Al. The results are found to be in good agreement with the total-energy calculations and experiment.

The rest of the paper is organized as follows. In Sec. II the generalized multiple-κ LMTO basis set is reviewed and the expressions for the Hamiltonian and overlap matrices are given in Sec. III. Section IV deals with the technique of computing the integrals over the interstitial region and the construction of polyhedra. In Sec. V we derive the formulas for atomic forces while the results of the frozen-phonon calculations are presented in Sec. VI. Section VII concludes the paper.

II. LINEAR MUFFIN-TIN ORBITALS

We shall first review the construction of linear muffin-tin orbitals. Space is partitioned into some polyhedral cell envelopes attributed to every atom. For these polyhedra we introduce inscribed muffin-tin spheres and also circumscribed spheres centered at the nuclei. Consider the so-called envelope function which is a singular Hankel function, $K_{\kappa L}(\mathbf{r}_R-\mathbf{t})$, centered at site $\mathbf{R}+\mathbf{t}$, as shown in Fig. 1(a), and has an energy $\varepsilon=\kappa^2$. (Here and in the following we assume that all radial functions with vector notations in brackets are multiplied by spherical harmonics where L denotes the combined index for lm; the lower subscript R for $\mathbf{r}$ denotes the difference $\mathbf{r}-\mathbf{R}$, where $\{\mathbf{R}\}$ are the positions of atoms in the unit cell while $\{\mathbf{t}\}$ are the primitive translations.) Inside its own sphere centered at $\mathbf{R}+\mathbf{t}$ we substitute the divergent part of the envelope function by a linear combination of numerical radial functions with the condition of smooth augmentation at the sphere boundary. The radial functions here are the solutions of the Schrödinger equation, $\phi_{RL}(\mathbf{r}_R-\mathbf{t},\varepsilon_{\nu\kappa Rl})$, with the spherically symmetric part of the potential as well as their energy derivatives, $\dot{\phi}_{RL}(\mathbf{r}_R-\mathbf{t},\varepsilon_{\nu\kappa Rl})$, taken for the energies $\varepsilon_{\nu\kappa Rl}$ at the centers of interest. Inside any other polyhedron centered at $\mathbf{R}'+\mathbf{t}'$ we substitute the tail of the envelope function by its expansion in terms of Bessel functions, i.e.,

$$K_{\kappa L}(\mathbf{r}_R-\mathbf{t})=\sum_{L'} J_{\kappa L'}(\mathbf{r}_{R'}-\mathbf{t}')S_{R'L'RL}(\mathbf{t}'-\mathbf{t},\kappa)\ , \qquad (1)$$

where $J_{\kappa L}(\mathbf{r}_R-\mathbf{t})$ is a Bessel function and $S_{R'L'RL}(\mathbf{t},\kappa)$ stands for the usual structure constants in direct space. [This is illustrated in Fig. 1(b).] The following definitions are accepted for Hankel and Bessel functions:

$$K_{\kappa l}(r)=-\frac{i(\kappa w)^{l+1}}{(2l-1)!!}h_l(\kappa r)\ , \qquad (2)$$

$$J_{\kappa l}(r)=\frac{1}{2}\frac{(2l-1)!!}{(\kappa w)^l}j_l(\kappa r)\ , \qquad (3)$$

where $h_l=j_l-in_l$ are the spherical Hankel functions and j_l, n_l are the spherical Bessel and Neuman functions. The expression for structure constants, then, is given by

$$S_{R'L'RL}(\mathbf{t},\kappa)=\sum_{L''}\frac{8\pi(2l''-1)!!}{(2l'-1)!!(2l-1)!!}C_{LL'}^{L''}(\kappa w)^{l+l'-l''}\times K_{\kappa l}(|\mathbf{t}-\mathbf{R}'+\mathbf{R}|)(-i)^{l''}\times Y_{L''}^{*}(\mathbf{t}-\mathbf{R}'+\mathbf{R})\ , \qquad (4)$$

where w is the average Wigner-Seitz radius and $C_{LL'}^{L''}$ are the Gaunt coefficients. The LMTO's are now arrived at by augmenting the Bessel functions in all MT spheres with linear combinations of ϕ_{RL} and $\dot{\phi}_{RL}$ [Fig. 1(c)] chosen such that the LMTO is everywhere continuous and differentiable.

The last step is to perform lattice summation of LMTO's centered at different sites with phase shifts $e^{i\mathbf{kt}}$ in order to guarantee that our basis functions would satisfy the Bloch theorem. This can be done trivially by producing the lattice Fourier transformation for structure constants (5) because the constructed orbitals are already represented everywhere as one-center expansions. Finally, we obtain our basis functions in the form

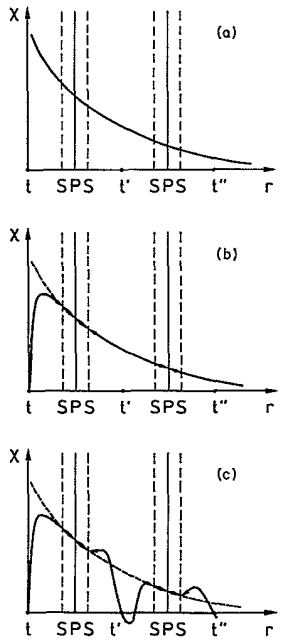

FIG. 1. Construction of the muffin-tin orbital: (a) the original envelope function, (b) substitution of the divergent part in the MT sphere at the origin by the linear combination of numerical radial functions and regular Bessel's function as well as substitution in all other (except the origin) polyhedra of the tail by its one-center expansion in Bessel's functions (illustrated by arrows), (c) substitution of Bessel's functions in all MT spheres by numerical radial functions. Vertical lines show the boundaries s of the MT spheres and the polyhedra.

$$\chi^{\mathbf{k}}_{\kappa RL}(\mathbf{r}_{R'})=\begin{cases}\Phi^{K}_{\kappa RL}(\mathbf{r}_R)\delta_{RR'}+\sum\limits_{L'}\Phi^{J}_{\kappa R'L'}(\mathbf{r}_{R'})S^{\mathbf{k}}_{R'L'RL}(\kappa) & \text{for } r_{R'}<s_{R'} \\ K_{\kappa L}(\mathbf{r}_R)\delta_{RR'}+\sum\limits_{L'}J_{\kappa L'}(\mathbf{r}_{R'})S^{\mathbf{k}}_{R'L'RL}(\kappa) & \text{for } \mathbf{r}_{R'}\in\Omega^{\text{int}}_{R'}\end{cases}, \tag{5}$$

where s_R are the MT-sphere radii and $S^{\mathbf{k}}_{R'L'RL}(\kappa)$ stands for the Fourier transformed structure constants (4):

$$S^{\mathbf{k}}_{R'L'RL}(\kappa)=\sum_{\mathbf{t}} e^{i\mathbf{k}\mathbf{t}}S^{\mathbf{k}}_{R'L'RL}(\mathbf{t},\kappa)\ . \tag{6}$$

The radial functions $\Phi^{K}_{\kappa RL}(r_R)$, $\Phi^{J}_{\kappa RL}(r_R)$ here are such linear combinations of the solutions ϕ_{RL} and $\dot{\phi}_{RL}$ which match smoothly to the Hankel and Bessel functions at the sphere boundary. We note that subscript κ in all potential dependent quantities follows merely from the fact that we can choose different centers of linearization $\varepsilon_{\nu\kappa Rl}$ depending on the tail energies.

Some comments should be made on the expansions (5). Inside nonoverlapping MT spheres they are rapidly convergent and not too complicated to evaluate. On the other hand, in the interstitial region Ω^{int}_R, belonging to a given atom, these expansions are badly convergent and valid only for $\mathbf{r}_R$ being less than the distance between nearest sites. This, in particular, means that our partition of space should generate polyhedra close to the compact Wigner-Seitz cells of close-packed structures in which the ratio between $\mathbf{r}_R\in\Omega^{\text{int}}$ and nearest-site distances is only about $\frac{1}{2}$. In the case of open structures the empty-sphere technique[13] should be used, first, in order to remove the areas where the one-center expansion diverges and, second, to diminish the number of terms in sums over L appearing in (5). In applications to frozen-phonon calculations we found that reducing the summation up to $l_{\max}=8$ always gives the convergence of phonon frequencies better than 1%. Specifically, for Al and Si with two empty spheres this accuracy is reached with $l_{\max}=6$ and for Nb having an essential d character of valence states, $l_{\max}=8$ should be used.

Let us discuss the choice of fixed tail energies $\varepsilon=\kappa^2$. In the original paper on the LMTO method[6] a $\kappa^2=0$ approximation is used and all formulas become particularly simple. This is possible because for close-packed structures the average kinetic energy for valence and conduction electrons is approximately zero within the window of $\simeq 1$ Ry. The systems we are interested in are distorted lattices in which the interstitial region must be accounted for more accurately. Many approaches are known for improving the LMTO basis set.[14] We should mention one[15] which became popular[16] where the size of the basis is increased by using more than one κ. While the first κ^2 is usually placed near the average potential in the interstitial region (so-called MT zero) the second and, possibly, third ones are taken to be large and negative (about -1 to -2 Ry). This has the advantage of improving the variational freedom of the basis by including some linear-combination-of-atomic-orbitals- (LCAO) type orbitals but has the disadvantage that increasing the LMTO set by threefold makes computer programs running 27 times slower.

The procedure we will follow is to use one (possibly two) κ value placed somewhere in the occupied part of the band and this choice follows from the energy-dependent KKR scattering theory. It is implemented for materials with the width of valence band ≤ 0.6–0.8 Ry where we expect that $\partial K/\partial\kappa$ and $\partial^2 K/\partial\kappa^2$ terms in the expansion would be small. In case of materials with wide valence bands or if MT spheres are very small, two-κ basis sets should be used and corresponding tail energies can be placed near the bottom and top of the band at a distance ≥ 0.8–1.0 Ry. (Smaller distances can lead to almost linearly dependent muffin-tin orbitals and a singular overlap matrix.)

In any case we come to the positive κ choice instead of the negative one and this can create some numerical problems. The problem is that using tail energies >0 makes structure constants singular when κ^2 is equal to free-electron energies. This singularity also occurs for $\mathbf{k}=0$ in the standard LMTO method which may be avoided by stepping out from the Γ point by a small vector. Here, we can, formally, consider $\varepsilon=\kappa^2$ a complex number, and adding some small imaginary part (usually a few hundredths of a Rydberg) removes this technical difficulty from the calculation.

III. HAMILTONIAN AND OVERLAP MATRIX

With the LMTO basis set defined in (5) the wave functions $\psi_{\mathbf{k}\lambda}(\mathbf{r})$ for valence electrons (the subscript λ enumerates the bands) are represented as linear combinations of $\chi^{\mathbf{k}}_{\kappa RL}(\mathbf{r})$ with the coefficients $A^{\mathbf{k}\lambda}_{\kappa RL}$ obtained from the variational principle. For the one-electron Hamiltonian given by local density-functional theory they are found from the eigenvalue problem

$$\sum_{\kappa RL}\left[\langle\chi^{\mathbf{k}}_{\kappa' R'L'}|-\nabla^2+V^{\text{MT}}(\mathbf{r})+V^{\text{NMT}}(\mathbf{r})|\chi^{\mathbf{k}}_{\kappa RL}\rangle-\varepsilon_{\mathbf{k}\lambda}\langle\chi^{\mathbf{k}}_{\kappa' R'L'}|\chi^{\mathbf{k}}_{\kappa RL}\rangle\right]A^{\mathbf{k}\lambda}_{\kappa RL}\equiv\sum_{\kappa RL}\left(H^{\mathbf{k}}_{\kappa' R'L'\kappa RL}-\varepsilon_{\mathbf{k}\lambda}O^{\mathbf{k}}_{\kappa' R'L'\kappa RL}\right)A^{\mathbf{k}\lambda}_{\kappa RL}=0\ , \tag{7}$$

where $V^{\text{MT}}(\mathbf{r})$ stands for the spherical and $V^{\text{NMT}}(\mathbf{r})$ for nonspherical parts of the potential. We now separate the contributions going from different space regions and write down the Hamiltonian matrix in the form

$$H^{\mathbf{k}}_{\kappa' R'L'\kappa RL}=H^{\mathbf{k},\text{MT}}_{\kappa' R'L'\kappa RL}+H^{\mathbf{k},\text{NMT}}_{\kappa' R'L'\kappa RL}+\kappa^2 O^{\mathbf{k},\text{int}}_{\kappa' R'L'\kappa RL}+V^{\mathbf{k},\text{int}}_{\kappa' R'L'\kappa RL} \tag{8}$$

and the overlap matrix in the form

$$O^{\mathbf{k}}_{\kappa' R' L' \kappa R L} = O^{\mathbf{k},\mathrm{MT}}_{\kappa' R' L' \kappa R L} + O^{\mathbf{k},\mathrm{int}}_{\kappa' R' L' \kappa R L} \ , \tag{9}$$

where the first and second terms in (8) and the first term in (9) denote the integrals over muffin-tin spheres and the others integrals over the interstitial, namely, $H^{\mathbf{k},\mathrm{MT}}_{\kappa' R' L' \kappa R L}$ is the matrix element of the operator $-\nabla^2 + V^{\mathrm{MT}}(\mathbf{r})$ and $H^{\mathbf{k},\mathrm{NMT}}_{\kappa' R' L' \kappa R L}$ is the nonspherical-potential matrix element. The third term in (8) is the matrix element of kinetic energy in the interstitial region. Since our basis functions here are the solutions of Helmholtz's equation it is trivially expressed through the interstitial overlap integral [second term in (9)]. The last term in (8) is the interstitial-potential matrix element.

All these contributions are represented as sum of one-, two-, and three-center integrals and we now give the expressions for them. The MT part of the Hamiltonian is

$$\begin{aligned} H^{\mathbf{k},\mathrm{MT}}_{\kappa' R' L' \kappa R L} = {} & \delta_{R' R} \delta_{L' L} \langle \Phi^K_{\kappa' R L} | -\nabla^2 + V^{\mathrm{MT}} | \Phi^K_{\kappa R L} \rangle_{s_R} + S^{\mathbf{k}*}_{R L R' L'}(\kappa') \langle \Phi^J_{\kappa' R L} | -\nabla^2 + V^{\mathrm{MT}} | \Phi^K_{\kappa R L} \rangle_{s_R} \\ & + \langle \Phi^K_{\kappa' R' L'} | -\nabla^2 + V^{\mathrm{MT}} | \Phi^J_{\kappa R' L'} \rangle_{s_{R'}} S^{\mathbf{k}}_{R' L' R L}(\kappa) \\ & + \sum_{R'' L''} S^{\mathbf{k}*}_{R'' L'' R' L'}(\kappa') \langle \Phi^J_{\kappa' R'' L''} | -\nabla^2 + V^{\mathrm{MT}} | \Phi^J_{\kappa R'' L''} \rangle_{s_{R''}} S^{\mathbf{k}}_{R'' L'' R L}(\kappa) \end{aligned} \tag{10}$$

and the MT part of the overlap matrix is

$$\begin{aligned} O^{\mathbf{k},\mathrm{MT}}_{\kappa' R' L' \kappa R L} = {} & \delta_{R' R} \delta_{L' L} \langle \Phi^K_{\kappa' R L} | \Phi^K_{\kappa R L} \rangle_{s_R} + S^{\mathbf{k}*}_{R L R' L'}(\kappa') \langle \Phi^J_{\kappa' R L} | \Phi^K_{\kappa R L} \rangle_{s_R} + \langle \Phi^K_{\kappa' R' L'} | \Phi^J_{\kappa R' L'} \rangle_{s_{R'}} S^{\mathbf{k}}_{R' L' R L}(\kappa) \\ & + \sum_{R'' L''} S^{\mathbf{k}*}_{R'' L'' R' L'}(\kappa') \langle \Phi^J_{\kappa' R'' L''} | \Phi^J_{\kappa R'' L''} \rangle_{s_{R''}} S^{\mathbf{k}}_{R'' L'' R L}(\kappa) \ . \end{aligned} \tag{11}$$

These formulas are simple generalizations of those used in the standard LMTO method.[6] All potential parameters may now be complex because a general, complex κ is assumed and the structure constants are no longer Hermitian. The radial matrix elements are calculated using the properties of the radial Schrödinger equation and its energy derivative. For $\kappa' = \kappa$ they are given by formulas (2.4) and (2.6) in Ref. 6. For $\kappa' \neq \kappa$ they are expressed through the values and slopes of radial functions at the sphere which is trivially derived from the Green second identity.[15]

The interstitial overlap matrix element is a two-center-type integral expressed via the product of two Hankel functions centered at sites $\mathbf{R}$ and $\mathbf{R}'$. Being eigenfunctions of ∇^2 they may be reexpanded in Bessel functions. This gives rise to the expansions (5) which are formally infinite. While these one-center expansions can be used to evaluate the integral with the technique described below in this paper, it complicates the determination of the overlap matrix. A better way is to use multicenter expansions and calculate the interstitial overlap matrix analytically in terms of the Green second theorem.[17] The final result in case $(\kappa'^2)^* = \varepsilon'^* \neq \kappa^2 = \varepsilon$ is

$$\begin{aligned} O^{\mathbf{k},\mathrm{int}}_{\kappa' R' L' \kappa R L}(\varepsilon - \varepsilon'^*) = {} & \delta_{R' R} \delta_{L' L} W_R \{ K^*_{\kappa' l} K_{\kappa l} \} + S^{\mathbf{k}*}_{R L R' L'}(\kappa') W_R \{ J^*_{\kappa' l} K_{\kappa l} \} + W_{R'} \{ K^*_{\kappa' l'} J_{\kappa l'} \} S^{\mathbf{k}}_{R' L' R L}(\kappa) \\ & + \sum_{R'' L''} S^{\mathbf{k}*}_{R'' L'' R' L'}(\kappa') W_{R''} \{ J^*_{\kappa' l''} J_{\kappa l''} \} S^{\mathbf{k}}_{R'' L'' R L}(\kappa) \ . \end{aligned} \tag{12}$$

In case $\varepsilon'^* = \varepsilon$ the result is

$$\begin{aligned} O^{\mathbf{k},\mathrm{int}}_{\kappa R' L' \kappa R L} = {} & \delta_{R' R} \delta_{L' L} W_R \{ K_{\kappa l} \dot{K}^*_{\kappa l} \} + \frac{i}{2} \omega \dot{S}^{\mathbf{k}*}_{R L R' L'}(\kappa) + S^{\mathbf{k}*}_{R L R' L'}(\kappa') W_R \{ K_{\kappa l} \dot{J}^*_{\kappa l} \} + W_{R'} \{ J_{\kappa l'} \dot{K}^*_{\kappa l'} \} S^{\mathbf{k}}_{R' L' R L}(\kappa) \\ & + \sum_{R'' L''} S^{\mathbf{k}*}_{R'' L'' R' L'}(\kappa') W_R \{ J_{\kappa l''} \dot{J}^*_{\kappa l''} \} S^{\mathbf{k}}_{R'' L'' R L}(\kappa) \ , \end{aligned} \tag{13}$$

where dots in all the quantities stand for the energy derivative. We have also used the compact Wronskian notations, $W_R\{f,g\} \equiv s_R^2 [f(s_R) g'(s_R) - g(s_R) f'(s_R)]$, which are defined at the sphere boundary.

The last step is to calculate the non-muffin-tin corrections to the Hamiltonian given by matrices $H^{\mathbf{k},\mathrm{NMT}}_{\kappa' R' L' \kappa R L}$ and $V^{\mathbf{k},\mathrm{int}}_{\kappa' R' L' \kappa R L}$. The first matrix is the NMT contribution within MT space, i.e.,

$$\begin{aligned} H^{\mathbf{k},\mathrm{NMT}}_{\kappa' R' L' \kappa R L} = {} & \delta_{R' R} \langle \Phi^K_{\kappa' R L'} | V^{\mathrm{NMT}} | \Phi^K_{\kappa R L} \rangle_{s_R} + \sum_{L''} S^{\mathbf{k}*}_{R L R' L'}(\kappa') \langle \Phi^J_{\kappa' R L''} | V^{\mathrm{NMT}} | \Phi^K_{\kappa R L} \rangle_{s_R} \\ & + \sum_{L''} \langle \Phi^K_{\kappa' R' L'} | V^{\mathrm{NMT}} | \Phi^J_{\kappa R' L''} \rangle_{s_{R'}} S^{\mathbf{k}}_{R' L' R L''}(\kappa) + \sum_{L'' L''' R''} S^{\mathbf{k}*}_{R'' L'' R' L'}(\kappa') \langle \Phi^J_{\kappa' R'' L''} | V^{\mathrm{NMT}} | \Phi^J_{\kappa R'' L'''} \rangle_{s_{R''}} S^{\mathbf{k}}_{R'' L''' R L}(\kappa) \ . \end{aligned} \tag{14}$$

The matrix elements here are reduced to the numerical radial integrals combined with the Gaunt coefficients as follows from the addition theorem for spherical harmonics and can be calculated explicitly. The second matrix is the interstitial potential contribution to the Hamiltonian calculated in terms of one-center expansions for LMTO's in the interstitial region. It is given by

$$V^{\mathbf{k},\mathrm{int}}_{\kappa R'L'\kappa RL}=\delta_{R'R}\langle K_{\kappa L'}|V|K_{\kappa L}\rangle_{\Omega^{\mathrm{int}}_R}+\sum_{L''}S^{\mathbf{k}*}_{RL''R'L'}(\kappa')\langle J_{\kappa L''}|V|K_{\kappa L}\rangle_{\Omega^{\mathrm{int}}_R}+\sum_{L''}\langle K_{\kappa' L'}|V|J_{\kappa L''}\rangle_{\Omega^{\mathrm{int}}_{R'}}S^{\mathbf{k}}_{R'L'RL''}(\kappa)$$
$$+\sum_{L''L'''R''}S^{\mathbf{k}*}_{R''L''R'L'}(\kappa')\langle J_{\kappa' L''}|V|J_{\kappa L'''}\rangle_{\Omega^{\mathrm{int}}_{R''}}S^{\mathbf{k}}_{R''L'''RL}(\kappa)\ , \tag{15}$$

where all the matrix elements are taken over the region between the MT sphere and the polyhedron boundary. In the following section we shall describe the method for calculating these integrals but now we discuss the expressions obtained. First, we see that non-muffin-tin corrections from inside the spheres and from the interstitial have the same form and can be treated together. They both are divided into $\mathbf{k}$-dependent structure constants and a potential-dependent part. The latter can be calculated once before the cycle over a mesh in $\mathbf{k}$ space and, consequently, the effort in producing the Hamiltonian lies only in performing the convolutions of radial matrix elements with the S matrix. The one-center expansions (5) converge inside MT spheres with $l_{\max}\leq 4$ and in the interstitial region with $l_{\max}\leq 8$. This means that single and double sums in the two- and three-center integrals must include higher angular momenta. The execution time we estimated in this case is approximately equal to solving the eigenvalue problem and thus for single-κ basis sets the total computing time taken on the preparation of H and O matrices with the subsequent diagonalization procedure is only 2–2.5 times slower compared to the standard LMTO-ASA calculations.

The potential $V(\mathbf{r})=V^{\mathrm{MT}}(\mathbf{r})+V^{\mathrm{NMT}}(\mathbf{r})$ in (15) is assumed to be expanded in spherical harmonics both inside the MT spheres and in the interstitial region. Its exchange-correlation part is found by supposing that nonspherical terms of the charge density are small. Then, we are able to use Taylor series for exchange-correlation formulas given by the LDA and find its spherical harmonics expansion within a sphere circumscribing the polyhedron. The Coulomb contribution is calculated by solving the Poisson equation inside the circumscribed spheres. The outer space can be accounted for if we know the multipole charges in each polyhedron. They are defined as integrals with the charge density multiplied by $r^l Y_L(\hat{\mathbf{r}})$ and can be calculated using the technique described below.

IV. INTERSTITIAL INTEGRALS

The preceding section gives a generalization of the LMTO method for a potential of arbitrary shape. Via the use of one-center expansions for LMTO's in the interstitial region we come to the problem of integrating the interstitial-potential matrix elements over the region between MT spheres and the plane boundaries of an atomic polyhedron. A related problem is to solve Poisson's equation in all space where it is necessary to integrate the charge density with a factor given by solutions of the Laplace equation.

A scheme performing these integrals has been proposed in Ref. 7 and then implemented in Ref. 4 concerning the full-potential KKR multiple scattering theory. It includes the expansion in spherical harmonics of the interstitial step function $\theta(\mathbf{r})$ which is unity in the interstitial region and zero elsewhere. Integrals may therefore be treated merely as numerical radial integrals taken over a sphere circumscribing the polyhedron. While this θ-function-expansion technique makes this scheme efficient and accurate, calculation of radial L components for $\theta(\mathbf{r})$ including the integration of a spherical harmonic over the complex region (part of a sphere of radius r lying inside the atomic polyhedron) complicates it. A better way is to reduce the volume integrals to surface ones in which plane boundaries of the polyhedron are very suitable for triangulation and which can be performed in terms of the standard two-dimensional quadrature formulas.[18]

We start from a formal rewriting of the integrand, which we generally denote as $f(r)Y_L(\hat{\mathbf{r}})$ in terms of the divergency of a vector field $\mathbf{r}F(r)Y_L(\hat{\mathbf{r}})/r^3$ where $F(r)$ stands for the first image of the radial function $f(r)$, i.e.,

$$F(r)=\int_a^r f(r')r'^2dr'\ , \tag{16}$$

where a is some lower limit. Applying the Gauss theorem we reduce the integral over the volume Ω_{int} to the surface S_{pol} of the polyhedron and sphere s:

$$\int_{\Omega_{\mathrm{int}}}f(r)Y_L(\hat{\mathbf{r}})d\mathbf{r}=\int_{S_{\mathrm{pol}}}\mathbf{r}F(r)Y_L(\hat{\mathbf{r}})/r^3d\mathbf{S}$$
$$-\sqrt{4\pi}F(s)\delta_{L0}\ , \tag{17}$$

where the last term is important only for the s harmonic because the integrals over any inner sphere for other harmonics are obviously equal to zero.

This approach is still too complicated for practical applications because we have to perform a complicated surface integration (17) for each function $f(r)$ of interest. However, most of these quantities have weak radial dependence in the interstitial region, first, because of the smallness of the latter (a few tenths of an Å in linear scale) and, second, because the wave functions of valence electrons here are plane waves with a characteristic wavelength of the order of a few Å. Consequently, we can use any interpolation in the interstitial region given between s and s_c, where s_c is the circumscribed sphere radius, by polynomial series. (Chebyshev's series used in this work usually produce an accuracy better than 10^{-10} by using the first ten terms.) We write

$$f(r)=\sum_n T_n(x)A^f_n\ , \tag{18}$$

where $T_n(x)$ is a Chebyshev polynomial of n order with an argument $x=(2r-s-s_c)/(s-s_c)$ and A^f_n are the expansion coefficients found from the well-known orthogonality properties of Chebyshev's polynomials. The next step is obvious. We introduce for convenience the following surface constants:

$$R_{nL}=\int_{\Omega_{\rm int}} r^n Y_L(\hat{\mathbf{r}})d\mathbf{r}$$
$$=\int_{S_{\rm pol}}\frac{r^n}{n+3}Y_L(\hat{\mathbf{r}})\mathbf{r}\,d\mathbf{S}-\sqrt{4\pi}\frac{s^{n+3}}{n+3}\delta_{L0}\,, \quad (19)$$

related to the power series r^n. Since R_{nL} depend only on the type of crystalline structure and, in particular, on our polyhedron partition they can be calculated once and saved on disk. Moreover, the surface constants

$$T_{nL}=\int_{\Omega_{\rm int}} T_n(x)Y_L(\hat{\mathbf{r}})d\mathbf{r}\,, \quad (20)$$

related to the Chebyshev series, as well as surface constants determined for different products of Chebyshev's polynomial with spherical harmonic, i.e.,

$$T_{n'L'nL}=\int_{\Omega_{\rm int}} T_{n'}(x)Y^*_{L'}(\hat{\mathbf{r}})T_n(x)Y_L(\hat{\mathbf{r}})d\mathbf{r}\,, \quad (21)$$

$$T^{n''L''}_{n'L'nL}=\int_{\Omega_{\rm int}} T_{n'}(x)Y^*_{L'}(\hat{\mathbf{r}})T_{n''}(x)Y_{L''}(\hat{\mathbf{r}})T_n(x)Y_L(\hat{\mathbf{r}})d\mathbf{r} \quad (22)$$

can be readily expressed through R_{nL} because any polynomial product is again a polynomial and any product of spherical harmonics is again a spherical harmonic.

With the above definitions we can write down the expressions for the interstitial integrals with one, two, and three functions having one-center spherical harmonics expansions in the form

$$\int_{\Omega_{\rm int}} g(\mathbf{r})d\mathbf{r}=\sum_{nL} A^g_{nL}T_{nL}\,, \quad (23)$$

$$\int_{\Omega_{\rm int}} g^*(\mathbf{r})h(\mathbf{r})d\mathbf{r}=\sum_{\substack{n'L'\\nL}} A^{g*}_{n'L'}T_{n'L'nL}A^h_{nL}\,, \quad (24)$$

$$\int_{\Omega_{\rm int}} g^*(\mathbf{r})v(\mathbf{r})h(\mathbf{r})d\mathbf{r}=\sum_{\substack{n'L'\\nL}} A^{g*}_{n'L'}\times\left[\sum_{n''L''}T^{n''L''}_{n'L'nL}A^V_{n''L''}\right]A^h_{nL}\,, \quad (25)$$

where A^g_{nL}, A^h_{nL}, and A^V_{nL} are the Chebyshev expansion coefficients found for L-radial components of functions $g(\mathbf{r})$, $h(\mathbf{r})$,and $v(\mathbf{r})$, respectively. By identifying function $g(\mathbf{r})$ with the charge density in expression (23) we obtain the formula for interstitial charge. By identifying the function $g(\mathbf{r})$ with the charge density and function $h(\mathbf{r})$ with regular solutions of the Laplace equation in expression (24) we obtain the formula for calculating multipole charges. At last, by identifying functions $g(\mathbf{r})$, $h(\mathbf{r})$ with Bessel and (or) Hankel functions and $v(\mathbf{r})$ with the full potential in expression (25) we obtain the formula for calculating the interstitial-potential matrix elements.

In order to obtain the complete scheme for the integration we, finally, give an algorithm for the construction of polyhedra. We want to describe crystalline space as a sum of some polyhedral areas attributed to every atom. Let us discuss carrying out this tesselation by the well-known Wigner-Seitz (WS) procedure. We plot the planes that lie perpendicular to the lines connecting a site at the origin with its different neighbors and divide these lines in the ratio 1:1. Thus we surround each atom with an arbitrary cell envelope called the Wigner-Seitz cell (for Bravae's lattice) or the Voronoi polyhedron (for disordered systems).

While valid in principle such a partition does not take into account the following circumstance. In the muffin-tin tesselation we introduce nonoverlapping spheres which surround every atom in the lattice. Formally, relations between their radii may be arbitrary. Indeed it is clear that the spheres must contain regions where the one-electron potential sharply changes and where, on the other hand, Schrödinger's equation can be solved most accurately. The WS procedure produces MT spheres inscribed in the polyhedra of fixed radii (which depend only on the distances between nearest sites) and, consequently, does not take into account the nature of the constituents involved.

The algorithm we want to find can be illustrated in the following manner. Consider three different atoms placed at the corners of an arbitrary triangle. If we apply the WS procedure we divide this triangle in three different areas and determine MT-sphere radii [Fig. 2(a)]. On the other hand, if we fix the MT-sphere radii we can perform the partition illustrated in Fig. 2(b) which may be more preferable for our purposes. From Fig. 2(b), we also realize that the WS algorithm is generalized by the division of lines connecting different neighbors in the ratio chosen, say, from physical arguments.

Mathematically, any partition of crystalline space on the atom surrounded by arbitrary envelopes can be yielded by introducing a set of functions $A_i(\mathbf{r})$ associated with each site i. Then, the condition

$$A_i(\mathbf{r})\le A_j(\mathbf{r}) \quad \text{for all } j\neq i \quad (26)$$

determines nonoverlapping areas Ω_i which fill up the space without holes. The proof that the areas do not overlap can be obtained if we consider point $\mathbf{r}_0$ which belongs to regions Ω_i and Ω_j spontaneously. Then, from the conditions

$$\begin{aligned} &A_i(\mathbf{r}_0)\le A_j(\mathbf{r}_0)\,,\\ &A_j(\mathbf{r}_0)\le A_i(\mathbf{r}_0)\,, \end{aligned} \quad (27)$$

it follows that $A_i(\mathbf{r}_0)=A_j(\mathbf{r}_0)$ or $\mathbf{r}_0$ is a boundary point. The absence of holes is also obvious because there always

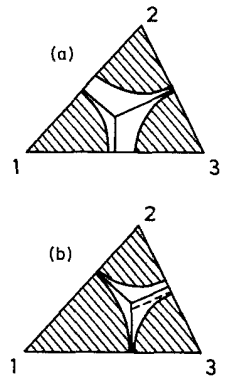

FIG. 2. (a) The illustrated Wigner-Seitz procedure and (b) an algorithm proposed for partitioning the space.

exists a minimum value

$$A_k(\mathbf{r})=\min_{j=1,2,\ldots}\{A_j(\mathbf{r})\} \tag{28}$$

for any r.

In the Wigner-Seitz case functions $A_i(\mathbf{r})$ are given by

$$A_i(\mathbf{r})=|\mathbf{r}-\mathbf{R}_i| \tag{29}$$

and (26) is written in the form

$$2\mathbf{r}(\mathbf{R}_j-\mathbf{R}_i)+R_i^2-R_j^2\leq 0\ . \tag{30}$$

This is the equation on boundaries and the solution of that is the WS cell or the Voronoi polyhedron. In the more general case in which we are interested, the equation on boundaries, $A_i(\mathbf{r})-A_j(\mathbf{r})=0$, should also [see Eq. (30)] have a form linear to r. This guarantees that our envelopes would be polyhedral ones. Let us introduce the following functions:

$$A_i(\mathbf{r})=-2\mathbf{R}_i\mathbf{r}+R_i^2+\beta_i\ . \tag{31}$$

We may conclude that the boundaries of such defined areas are the planes which lie perpendicular to the lines connecting neighbors. These lines are divided in the ratio

$$\alpha_{ij}=\frac{\beta_j-\beta_i}{2|\mathbf{R}_i-\mathbf{R}_j|^2}+\frac{1}{2}\ , \tag{32}$$

that is determined by some numbers β_i. By surrounding every atom with nonoverlapping spheres of radii s_i we also introduce the preferable ratio

$$\alpha_{ij}^p=\frac{s_i}{s_i+s_j} \tag{33}$$

and it is our purpose to find the connection between s_i and β_i. Of course, the relation (33) can, in principle, be only satisfied for sites with touching spheres [sites 1,2 and 1,3 in Fig. 2(b)] and, consequently, we cannot find this connection by direct comparison to the expressions (32) and (33). The number of free parameters β_i in this case will be less than the number of conditions. (The latter is estimated as the number of nearest sites.) Let us consider, on the other hand, the following relation:

$$\beta_i=-s_i^2\ . \tag{34}$$

Since $s_i+s_j=|\mathbf{R}_i-\mathbf{R}_j|$ for sites with touching spheres we conclude for them that $\alpha_{ij}=\alpha_{ij}^p$. Moreover, the equality (34) produces only "proper" polyhedral envelopes which means that the situation shown in Fig. 2(b) by dashed lines is never realized. This proves that the described algorithm can be used for polyhedron construction.

V. ATOMIC FORCES

Within density-functional theory the change in total energy due to displacements of atoms can now be computed using the full-potential LMTO method described above. This is the necessary step in the testing of the full-potential scheme and in the following section we give the results of such frozen-phonon calculations comparing with the LAPW, a pseudopotential, and another full-potential (FP) LMTO calculation as well as with the experiment. While this total-energy approach usually gives the percentage accuracy in the prediction of the phonon frequencies, it has great computational disadvantage in dealing with the difference of ~ 1 mRy between total energies which are themselves of the order of thousandths of Rydbergs. A better approach is to perform an analytical differentiation of the total energy with respect to the displacements of nuclei, and calculate the atomic forces, which have to be much more accurate.

According to the Hellman-Feynman (HF) theorem the force on an atom is the electrostatic force on its nucleus and, consequently, uniquely determined by the electronic charge distribution in crystal. Unfortunately, the latter quantity is usually constructed from the one-electron wave functions, being approximate solutions of Schrödinger's equation, and Hellman-Feynman forces may be highly inaccurate. Since, on the other hand, the atomic forces obtained numerically from the total-energy differentiation provide good results, an additional contribution to the HF force appears which is connected with using the incomplete basis-function set for representing wave functions. This is the so-called Pulay force[12] which vanishes in the full-potential KKR theory[19] or in the plane-wave pseudopotential calculations for materials with s,p electrons but must be taken into account in the all-electron LAPW- and LMTO-based methods.[20,22]

We shall now give the derivation for atomic forces within our formalism. We first write the total energy for a solid in the DFT framework by representing this quantity as the following sum:

$$E_{\rm tot}=T_{\rm val}+T_{\rm cor}+E_{\rm el}+E_{\rm xc}\ , \tag{35}$$

where $T_{\rm val}$, $T_{\rm cor}$ are the kinetic energies for valence and core electrons, $E_{\rm el}$ is the electrostatic (Hartree) energy including electron-electron, electron-nucleus, nucleus-nucleus interactions and $E_{\rm xc}$ is the exchange-correlation energy as given by LDA. The kinetic energy is usually expressed through the sum of one-electron energies minus the effective potential energy and for valence electrons is given by

$$T_{\rm val}=\sum_{\mathbf{k}\lambda} f_{\mathbf{k}\lambda}\varepsilon_{\mathbf{k}\lambda}-\sum_R\int_{\Omega_R}\rho_R^{\rm val}(\mathbf{r}_R)V_R(\mathbf{r}_R)d\mathbf{r}_R\ , \tag{36}$$

where $f_{\mathbf{k}\lambda}$ are the occupation numbers, $\rho_R^{\rm val}$, V_R are the valence charge density and the effective potential represented in our LMTO method as one-center expansions in every atomic polyhedron Ω_R, and the sum over R means the integration over the unit cell. For deep-lying core states their kinetic energy is

$$T_{\rm cor}=\sum_{iR} f_{iR}\varepsilon_{iR}-\sum_R\int_{s_R}\rho_R^{\rm cor}(r_R)V_R^{\rm MT}(r_R)d\mathbf{r}_R\ , \tag{37}$$

where f_{iR} is the occupation number for ith core level ε_{iR}; $\rho_R^{\rm cor}$ is the spherically symmetric core charge distribution in the Rth atom which vanishes outside its own MT sphere. [We assume that the core eigenstates are the exact solutions of Schrödinger's (Dirac's) equation with the spherical part $V^{\rm MT}$ of the potential. We also assume that higher-lying semicore states are treated as *valencelike*

states and have already been accounted for in (36).] The electrostatic energy connected with the full electronic densities $\rho_R=\rho_R^{\rm cor}+\rho_R^{\rm val}$ and nuclear charges Z_R is given by

$$E_{\rm el}=\frac{1}{2}\sum_R\int_{\Omega_R}\int[\rho_R(\mathbf{r}_R)+Z_R\delta(\mathbf{r}_R)]V_R^C(\mathbf{r}_R)d\mathbf{r}_R-E_0\ , \tag{38}$$

where V_R^C is the Coulomb potential in the Rth atomic polyhedron which can be written as follows:

$$V_R^C(\mathbf{r}_R)=-\frac{Z_Re^2}{r_R}+e^2\int_{\Omega_R}\frac{\rho_R(\mathbf{r}'_R)}{|\mathbf{r}_R-\mathbf{r}'_R|}d\mathbf{r}'_R+e^2\sum_L\left[\frac{r_R}{w}\right]^l i^lY_L(\hat{\mathbf{r}}_R)\frac{i\sqrt{\pi}w}{(2l+1)}\times\sum_{R'L'}S^{\mathbf{k}=0}_{R'L'RL}(\kappa=0)\frac{M_{R'L'}}{(2l'+1)}\ . \tag{39}$$

The first and second terms here are nuclear and electronic contributions from within a polyhedron and the last term is the Madelung potential. It is expressed via the standard structure constants for $\mathbf{k}$ and κ equal to zero and total multipole charges M_{RL} defined as

$$M_{RL}=-\delta_{L0}Z_R+\sqrt{4\pi}\int_{\Omega_R}\rho_R(\mathbf{r}_R)\left[\frac{r_R}{w}\right]^l[i^lY_L(\hat{\mathbf{r}}_R)]^*d\mathbf{r}_R\ . \tag{40}$$

We have also subtracted from the definition $E_{\rm el}$ the Coulomb energy of the nucleus by denoting this divergent quantity as E_0. The exchange-correlation energy in the LDA is given by

$$E_{\rm xc}=\sum_R\int_{\Omega_R}\rho_R(\mathbf{r}_R)\varepsilon_{\rm xc}(\mathbf{r}_R)d\mathbf{r}_R\ , \tag{41}$$

where $\varepsilon_{\rm xc}$ is the density of the exchange-correlation energy for homogeneous electron system with density ρ.

We will proceed with the derivation by performing the variation of every contribution to the total energy. We suppose that the initial atomic configuration inside the unit cell is given by positions $\{\mathbf{R}\}$. By allowing atoms to move slightly we come to the final geometry $\{\mathbf{R}+\delta\mathbf{R}\}$ where $\delta\mathbf{R}$ denotes the nuclear displacements. The change in charge density, $\delta\rho_R(\mathbf{r}_R)$, due to the presence of such frozen phonon (so-called electronic response) is the difference between self-consistent densities $\bar{\rho}_{R+\delta R}(\mathbf{r}_{R+\delta R})$ and $\rho_R(\mathbf{r}_R)$ for the final and initial configurations, respectively. Referring to the coordinate system of the initial state $\{\mathbf{R}\}$ we write $\delta\rho_R(\mathbf{r}_R)$ in the form (linear with respect to displacements)

$$\delta\rho_R(\mathbf{r}_R)=\delta^s\rho_R(\mathbf{r}_R)-\delta\mathbf{R}\nabla\rho_R(\mathbf{r}_R)\ , \tag{42}$$

where the first term is the "soft" contribution to the response which is the difference:

$$\delta^s\rho_R(\mathbf{r}_R)=\bar{\rho}_{R+\delta R}(\mathbf{r}_R)-\rho_R(\mathbf{r}_R)\ , \tag{43}$$

determined for the same origin while the second "rigid" term in (42) goes merely from the fact that our coordinate system is position dependent.

With these definitions the change in kinetic energy for the core electrons is written as follows:

$$\delta T_{\rm cor}=\sum_{iR}f_{iR}\delta\varepsilon_{iR}-\sum_R\int_{s_R}\rho_R^{\rm cor}(r_R)\delta V_R^{\rm MT}(r_R)d\mathbf{r}_R-\sum_R\int_{s_R}\delta^s\rho_R^{\rm cor}(r_R)V_R^{\rm MT}(r_R)d\mathbf{r}_R+\sum_R\delta\mathbf{R}\int_{s_R}\nabla\rho_R^{\rm cor}(r_R)V_R^{\rm MT}(r_R)d\mathbf{r}_R\ . \tag{44}$$

Since the one-electron core levels ε_{iR} are the exact eigenvalues of Schrödinger's (Dirac's) equation with the spherically symmetric part of the potential we simply get $\delta\varepsilon_{iR}=\langle iR|\delta V_R^{\rm MT}|iR\rangle$ as follows from the Hellman-Feynman theorem, where $|iR\rangle$ are the exact eigenfunctions for the core problem in the atom R, decaying outside its own MT sphere. Consequently, performing the summation over occupied states we see that the first and second contributions to $\delta T_{\rm cor}$ are ideally canceled out. Moreover, we are able to use the following property: $\langle iR|\nabla V_R^{\rm MT}|iR\rangle=0$, valid for exact eigenfunctions, which after summing over occupied states makes the last contribution to $\delta T_{\rm cor}$ also equal to zero. Thus we arrive at

$$\delta T_{\rm cor}=-\sum_R\int_{s_R}\delta^s\rho_R^{\rm cor}(r_R)V_R^{\rm MT}(r_R)d\mathbf{r}_R\ , \tag{45}$$

expressing the change in $T_{\rm cor}$ through the soft electronic response only.

The change in electrostatic and exchange-correlation energies is obtained directly by performing the variations of formulas (38) and (41). We also separate, for convenience, soft and rigid parts in the screening of nuclear displacements and after some tedious reorganizations come to the result

$$\delta E_{\rm el}=\sum_R\int_{\Omega_R}\delta^s\rho_R(\mathbf{r}_R)V_R^C(\mathbf{r}_R)d\mathbf{r}_R-\sum\delta\mathbf{R}\int_{\Omega_R}\nabla[\rho_R(\mathbf{r}_R)V_R^C(\mathbf{r}_R)]d\mathbf{r}_R-\sum\delta\mathbf{R}\mathbf{F}_R^M\ , \tag{46}$$

where all the integrals are taken over the surface of the polyhedron and where

$$\mathbf{F}_R^M=\frac{-ie^2w}{2}\sum_{LL'R'}\frac{M^*_{RL}}{(2l+1)}\left[\frac{d}{d\mathbf{R}}S^{\mathbf{k}=0}_{RLR'L'}(\kappa=0)\right]\times\frac{M_{R'L'}}{(2l'+1)} \tag{47}$$

is the Madelung force expressed via the change in the structure constants calculated explicitly. The exchange-correlation energy variation is given by

$$\delta E_{\rm xc}=\sum_R\int_{\Omega_R}\delta^s\rho_R(\mathbf{r}_R)V_R^{\rm xc}(\mathbf{r}_R)d\mathbf{r}_R-\sum_R\delta\mathbf{R}\int_{\Omega_R}\nabla[\rho_R(\mathbf{r}_R)\varepsilon_{\rm xc}(\mathbf{r}_R)]d\mathbf{r}_R\ , \tag{48}$$

where $V^{\rm xc}=d[\rho\varepsilon_{\rm xc}]/d\rho$ stands for the exchange-correlation potential.

We now must evaluate the change in kinetic energy for valence electrons. This is, in general, the most difficult

problem because our one-electron wave functions are necessarily approximate. We first produce the formal variation of (36) expressing $\delta T_{\rm val}$ via the change in valence density, effective potential, and one-electron energies, $\delta\varepsilon_{\mathbf{k}\lambda}$, i.e.,

$$\delta T_{\rm val}=\sum_{\mathbf{k}\lambda} f_{\mathbf{k}\lambda}\delta\varepsilon_{\mathbf{k}\lambda}-\sum_R \int_{\Omega_R}\rho_R^{\rm val}(\mathbf{r}_R)\delta V_R(\mathbf{r}_R)d\mathbf{r}_R$$
$$-\sum_R \int_{\Omega_R}\delta^s\rho_R^{\rm val}(\mathbf{r}_R)V_R(\mathbf{r}_R)d\mathbf{r}_R$$
$$+\sum_R \delta\mathbf{R}\int_{\Omega_R}\nabla\rho_R^{\rm val}(\mathbf{r}_R)V_R(\mathbf{r}_R)d\mathbf{r}_R\ . \qquad (49)$$

(The term containing the variation in occupation numbers vanishes as a result of the electron-number conservation condition.) One sees that supposing our valence eigenstates to be the exact solutions of Schrödinger's equation we will have $\delta\varepsilon_{\mathbf{k}\lambda}=\langle\mathbf{k}\lambda|\delta V|\mathbf{k}\lambda\rangle$ as a result of the Hellman-Feynman theorem and after summing over all occupied states the first and second terms in $\delta T_{\rm val}$ are canceled out. At this point we look at the change in total energy represented by the sum of contributions (45), (46), (48), and (49) and conclude that all the terms containing the soft density variation $\delta^s\rho$ simply give

$$V_0\sum_{\mathbf{R}}\delta\mathbf{R}\int_{\Omega_R}\nabla\rho_R(\mathbf{r}_R)d\mathbf{r}_R\ , \qquad (50)$$

where V_0 is just the zero of the energy scale (MT zero). This result is obtained if the charge density and the potential are self-consistent and since the total induced charge inside the unit cell is equal to zero because of the electroneutrality condition. We now add to and subtract from the total-energy variation the so-called core correction:

$$\delta E_c=-\sum_R\delta\mathbf{R}\int_{s_R}\nabla\rho_R^{\rm cor}(r_R)V_R(\mathbf{r}_R)d\mathbf{r}_R\ , \qquad (51)$$

defined with the full potential [instead of its MT part entered in (44)] and after combining all the terms with $\nabla\rho$ we also cancel out the contribution containing the rigid change in charge density. The final result reads as

$$(\delta E_{\rm tot})_{\rm HF}=\delta E_c$$
$$-\sum_R\delta\mathbf{R}\left[F_R^M+\int_{\Omega_R}\rho_R(\mathbf{r}_R)\nabla V_R^C(\mathbf{r}_R)d\mathbf{r}_R\right], \qquad (52)$$

where the expression in brackets is the so-called Hellman-Feynman force on an atom which is the electrostatic force on its nucleus. Together with the core corrected force the HF force is very sensitive to the behavior of the charge density near the nucleus and must be treated with care.

The result (52) for the total-energy variation following from the Hellman-Feynman theorem (we marked this fact by labeling $\delta E_{\rm tot}$ with abbreviation HF) assumes that our one-electron wave functions are the exact ones, i.e., $(-\nabla^2+V-\varepsilon_{\mathbf{k}\lambda})|\mathbf{k}\lambda\rangle\equiv 0$. On the other hand, these functions are found in terms of the variational principle and it is our purpose to obtain the expressions for the one-electron energy variation in this framework. We now perform the variation of the LMTO-eigenvalue problem (7) and get the relation for $\delta\varepsilon_{\mathbf{k}\lambda}$ in the form

$$\delta\varepsilon_{\mathbf{k}\lambda}=\sum_{\substack{\kappa'R'L'\\ \kappa RL}} A^{\mathbf{k}\lambda *}_{\kappa'R'L'}(\delta H^{\mathbf{k}}_{\kappa'R'L'\kappa RL}-\varepsilon_{\mathbf{k}\lambda}\delta O^{\mathbf{k}}_{\kappa'R'L'\kappa RL})A^{\mathbf{k}\lambda}_{\kappa RL} \qquad (53)$$

expressing it via the change in the Hamiltonian and overlap matrix only. Examining the expressions (10)–(15) for them we see that H and O matrices are functions of combinations of potential parameters and structure constants. The potential parameters depend on the numerical radial functions $\phi_{\kappa RL}$, $\dot\phi_{\kappa RL}$ and the change $\delta\phi_{\kappa RL}$, $\delta\dot\phi_{\kappa RL}$ in these is due to the rigid shift $-\delta\mathbf{R}\nabla V_R$ of the potential moved with the nucleus as well as the soft potential variation $\delta^s V_R$ being the difference between exact δV_R and $-\delta\mathbf{R}\nabla V_R$. While the rigid part in the screening potential will lead us to the following form: $-\delta\mathbf{R}\nabla\phi_{\kappa RL'}$, $-\delta\mathbf{R}\nabla\phi_{\kappa RL}$ for the change in radial functions, the solutions $\delta^s\phi_{\kappa RL}$, $\delta^s\dot\phi_{\kappa RL}$ connected with $\delta^s V_R$ are hard to calculate quickly. The main difficulty is in finding the soft potential variation which is expressed via $\delta^s\rho_R$ and, consequently, again via $\delta^s\phi_{\kappa RL}$, $\delta^s\dot\phi_{\kappa RL}$. One should use the linear response theory to find these quantities but this is impractical to do for the frozen-phonon calculations described here. We now neglect $\delta^s\phi$ and $\delta^s\dot\phi$ contributions (discussed below) in the variations $\delta H^{\mathbf{k}}_{\kappa'R'L'\kappa RL}$ and $\delta O^{\mathbf{k}}_{\kappa'R'L'\kappa RL}$ while the rest can be performed analytically (see the Appendix). Finally we obtain

$$\delta\varepsilon_{\mathbf{k}\lambda}=\langle\mathbf{k}\lambda|V|\mathbf{k}\lambda\rangle-\sum_R\delta R\int_{\Omega_R}V_R(\mathbf{r}_R)\nabla[\psi^*_{\mathbf{k}\lambda}(\mathbf{r}_R)\psi_{\mathbf{k}\lambda}(\mathbf{r}_R)]d\mathbf{r}_R$$
$$-\sum_{R_0}\delta\mathbf{R}_0\left\{-\sum_{\substack{\kappa'R'L'\\ \kappa RL}} A^{\mathbf{k}\lambda *}_{\kappa'R'L'}\left[\frac{d}{d\mathbf{R}_0}H^{\mathbf{k}}_{\kappa'R'L'\kappa RL}-\varepsilon_{\mathbf{k}\lambda}\frac{d}{d\mathbf{R}_0}O^{\mathbf{k}}_{\kappa'R'L'\kappa RL}\right]A^{\mathbf{k}\lambda}_{\kappa RL}\right\}, \qquad (54)$$

where $d/d\mathbf{R}$ means here that the differentiation in the structure constants needs only to be performed in the Hamiltonian and overlap matrix. This formula is the generalization of the Hellman-Feynman result (first term here) and the second and third contributions are the so-called incomplete basis-set corrections including a surface contribution found recently[22] in connection with the LAPW formalism. Using this relationship for the

definition $\delta\varepsilon_{\mathbf{k}\lambda}$ in formula (49) we conclude that the second and last terms in the change $\delta T_{\rm val}$ are combined with the first and second terms in (54) after summing over all occupied states and ideally canceled out. Thus the very impractical last contribution in $\delta T_{\rm val}$ disappeared and the resulting expression reads as

$$\delta T_{\rm val}=\sum_{\mathbf{k}\lambda} f_{\mathbf{k}\lambda}\sum_R \delta\mathbf{R}F_R^{\mathbf{k}\lambda} -\sum_R\int_{\Omega_R}\delta^s\rho_R^{\rm val}(\mathbf{r}_R)V_R(\mathbf{r}_R)d\mathbf{r}_R\ , \tag{55}$$

where $F_R^{\mathbf{k}\lambda}$ stands for the change in the eigenvalues connected with the change in the structure constants per unit displacement [the expression in $\{\ \}$ in the last term of (54)].

The change in the total energy is now given by the sum of expressions (45), (46), (48), and (55) and we again see that all the terms with the soft density variation simply give (50) if the self-consistency is reached. The total force is thus given by

$$\mathbf{F}_R^{\rm tot}=\sum_{\mathbf{k}\lambda} f_{\mathbf{k}\lambda}\mathbf{F}_R^{\mathbf{k}\lambda}+\mathbf{F}_R^M+\int_{\Omega_R}\nabla[\rho_R(\mathbf{r}_R)V_R^C(\mathbf{r}_R)]d\mathbf{r}_R +\int_{\Omega_R}\nabla[\rho_R(\mathbf{r}_R)\varepsilon_{\rm xc}(\mathbf{r}_R)]d\mathbf{r}_R -V_0\int_{\Omega_R}\nabla\rho_R(\mathbf{r}_R)d\mathbf{r}_R\ , \tag{56}$$

where the last three contributions are indeed the integrals over the surface of the polyhedron. The present result agrees with that given by the well-known Andersen force theorem[21] and expressed the force in terms of the change in the sum of the one-electron energies upon virtual displacements of frozen potentials plus the electrostatic and surface terms. Since all the surface integrals and $\mathbf{F}_R^M$ are calculated explicitly the only difficulty is to produce the change in the eigenvalues $\mathbf{F}_R^{\mathbf{k}\lambda}$ for every $\mathbf{k}$ point and band λ. We estimated that for this case the time is increased by 50% of that used for the solution of the eigenvalue problem and, consequently, the force calculations described here are fairly efficient.

We now take a closer look at the validity of approximations used in this derivation. The main assumption is neglect of $\delta^s\phi$, $\delta^s\dot\phi$ contributions at the calculation of the band energy variation $\delta\varepsilon_{\mathbf{k}\lambda}$. What we actually do is the estimation of the matrix element:

$$\langle\delta\chi^{\mathbf{k}}_{\kappa RL}|-\nabla^2+V-\varepsilon_{\mathbf{k}\lambda}|\mathbf{k}\lambda\rangle \tag{57}$$

which is obviously not zero if $|\mathbf{k}\lambda\rangle$ are found variationally. The change $\delta\chi^{\mathbf{k}}_{\kappa RL}$ in the muffin-tin orbital is the difference between the MT orbitals $\tilde\chi^{\mathbf{k}}_{\kappa R+\delta RL}$ and $\chi^{\mathbf{k}}_{\kappa RL}$ defined for the final and initial atomic configurations, respectively. The approximation is essentially that of substituting the exact orbital $\tilde\chi^{\mathbf{k}}_{\kappa R+\delta RL}$ by the orbital $\chi^{\mathbf{k}}_{\kappa R+\delta RL}$ constructed in terms of the solutions $\phi_{\kappa RL}$ and $\dot\phi_{\kappa RL}$ for the original crystal. This leads us to the rigid part in the change $\delta\chi^{\mathbf{k}}_{\kappa RL}$ which is $-\delta\mathbf{R}'\nabla\delta\chi^{\mathbf{k}}_{\kappa RL}(\mathbf{r}_{R'})$ in each (R')th polyhedron plus the contribution connected with the change in the structure constants only. This rigid part is used to estimate (57). The contribution which is not taken into account is the soft part $\delta^s\chi^{\mathbf{k}}_{\kappa RL}$ connected with the change $\delta^s\phi,\delta^s\dot\phi$. Since our trial functions in the interstitial region do not depend on the potential parameters the soft part is not equal to zero only inside the MT spheres. Consequently the error in the determination of forces is proportional to the following matrix element:

$$\langle\delta^s\chi^{\mathbf{k}}_{\kappa RL}|-\nabla^2+V-\varepsilon_{\mathbf{k}\lambda}|\mathbf{k}\lambda\rangle_{\Omega_{\rm MT}}\ , \tag{58}$$

where the volume of integration is the MT region and where the induced orbital $\delta^s\chi^{\mathbf{k}}_{\kappa RL}$ is zero and has zero derivative at the sphere boundary. We thus see that the errors are mainly connected with the linearized character of our MT orbitals and can be sufficiently small if the energy parameters are appropriately chosen.

VI. FROZEN-PHONON CALCULATIONS

In this section test results for the total-energy and force calculations of frozen phonons in Si, Nb, and Al are presented and compared with existing LAPW, pseudopotential, and another FP-LMTO calculations as well as with experiment. A few comments should be made on the calculation. First, for all the materials we use one-κ s-, p-, and d-muffin-tin orbitals for representing one-electron wave functions which makes the LMTO Hamiltonian and overlap matrices low dimensional. Second, since our method uses a one-center spherical harmonics expansion for the wave functions, charge density, and potential in the interstitial region we must include in the summation over l higher angular momenta. We use $l_{\rm max}=6-8$ (specified below) for the expansion of the tails of s, p, and d orbitals which implies the procedure of internal summation in two- and three-center integrals of the Hamiltonian as discussed in Sec. III. (The overlap matrix converges much more rapidly as a result of using multicenter expansions for LMTO's in the interstitial region.) Although, to reach the convergency of the total energy of ~ 1 mRy per atom one should use $l_{\rm max}=10-12$, the convergency of the energy difference between distorted and undistorted lattices or atomic forces calculated at a given atomic geometry is achieved at $l_{\rm max}=6-8$ which seems to be fairly sufficient for our purposes. The wave functions themselves are expanded

TABLE I. Calculated energy differences (mRy per cell) associated with the Γ-point phonon in Si for two distorted configurations $\pm(\frac{1}{8}-0.005+y)a(1,1,1)$ with respect to the configuration with $y=0$. For notations see text.

y	$\delta E_{\rm tot}$	$\delta T_{\rm val}$	$\delta T_{\rm cor}$	$\delta E_{\rm el}$	$\delta E_{\rm xc}$
+0.001 25	−2.445	−5.276	0.008	2.532	0.021
−0.001 25	3.203	8.730	−0.014	−4.851	−0.054

TABLE II. Calculated soft contributions to the energy variations associated with the Γ-point phonon in Si for two distorted configurations $\pm(\frac{1}{8}-0.005+y)a(1,1,1)$ with respect to the configuration with $y=0$. Notations are explained in text. Units are mRy per cell.

y	$\delta^s\rho^v V$	$\delta^s\rho^c V$	$\delta^s\rho V_C$	$\delta^s\rho V_{xc}$	$\delta^s\rho V_0$
+0.001 25	6.156	−0.008	5.878	2.586	2.396
−0.001 25	−9.195	0.014	−8.971	−4.149	−4.065

up to $l_{max}=4$ in all calculations while the charge density and potential are both expanded up to $l_{max}=8$. The last comment concerns the treatment of semicore states. Since MT spheres have to be kept the same for all distorted configurations of a given lattice and do not overlap they become sufficiently small. This requires the amplitudes of low-lying (~ -5 to -8 Ry) core states to have finite values at the sphere boundary. These states are all treated as the band states in the full potential and calculated in separate energy windows in the approximation of neglecting hybridization with valence states. The deep-lying core states, on the other hand, are found from the atomic calculations as the eigenvalues of Dirac's equation with the MT part of the potential and recalculated at each self-consistent iteration.

We now present the results of our calculations for the Γ-point optical phonon in Si. This mode is investigated by moving two silicon atoms along the (1,1,1) direction. The atomic geometries are given by the positions $\pm(\frac{1}{8}+x)a(1,1,1)$ where $a=10.26$ a.u. is the experimental lattice constant. As is standard practice when using the LMTO method an equal number of empty spheres is included along with the Si atoms. Their positions are also changed to keep a total number of symmetry operations (12) for all distorted configurations. The basis set for representing the wave functions has a one-center spherical harmonics expansion up to $l_{max}=6$. The fixed tail energy is chosen to be 0.1 Ry and has a small imaginary part equal to 0.03 Ry. $2s$- and $2p$-core states are also treated as the band states with tail energies of -9.4 and -6.4 Ry, respectively. All MT-sphere radii are taken as 2.10 a.u. The exchange-correlation potential of Ref. 23 is used and the tetrahedron method[24] is applied for Brillouin-zone (BZ) integration.

We first make a numerical analysis of different contributions to the atomic force at the configuration given by the positions $\pm(\frac{1}{8}+x)a(1,1,1)$ with $x=0.005$ in order to compare them with calculated forces after formula (56). For this purpose we use a small number (18) of **k** points for the BZ integration and calculate kinetic, electrostatic, and exchange-correlation energies for a number of atomic geometries $\pm(\frac{1}{8}+x+y)a(1,1,1)$ as functions of value y. Referencing to the initial configuration with $y=0$ we then compute the energy differences δE_{tot}, δT_{val}, δT_{cor}, δE_{el}, and δE_{xc} and the results of such calculations for two atomic geometries are given in Table I. From these data we may, in particular, conclude that the change in total energy is obtained as a result of delicate compensation of different contributions and no one term here can be neglected except maybe the change in kinetic energy for deep-lying core states. To derive numerically the atomic forces it is also necessary to compute the contributions to the energy variations (45), (46), (48), and (55) going from the soft change $\delta^s\rho$ in the charge density. This can be done trivially if the self-consistent densities are known for all y configurations by calculating $\delta^s\rho$ directly as the difference between ρ_y and $\rho_{y=0}$. Let us symbolically denote the integrals over the unit cell with the soft valence density variation and the potential as $\delta^s\rho^v V$, with the soft core density variation and the potential as $\delta^s\rho^c V$, with the soft total density variation and Coulomb part of the potential as $\delta^s\rho V_C$, exchange-correlation part of the potential as $\delta^s\rho V_{xc}$, and MT-zero constant potential as $\delta^s\rho V_0$. All these integrals are calculated for different y geometries relative to the configuration with $y=0$. Two of these calculations are presented in Table II. Using this analysis we are able to estimate numerically different contributions to the atomic force. Namely, we find the derivative with respect to the distortion given by value y of $\delta T_{val}+\delta^s\rho^v V$ to obtain [see formula (55)] the contribution connected with the change in the Hamiltonian and overlap matrices [the first term in (56) which is referred to hereafter as the band contribution to the atomic force, F_{bnd}]. The sum $\delta T_{cor}+\delta^s\rho^c V$ is

TABLE III. Comparison between calculated and numerical forces (notations are in text) for the atomic geometry $\pm(\frac{1}{8}-0.005)a(1,1,1)$ associated with the Γ-point phonon in Si. Units are Ry/a_B.

	F_{bnd}	F_{el}	F_{xc}	F_0	F_{tot}
Numerical forces	−0.015 89	0.084 11	0.064 87	−0.072 68	0.060 41
Cal. forces at Si atom	−0.014 14	0.082 63	0.062 31	−0.070 80	0.059 15
Calc. forces at empty site	−0.001 39	0.001 50	0.002 53	−0.001 84	0.000 81
Total calc. forces	−0.016 33	0.084 13	0.064 85	−0.072 69	0.059 96

TABLE IV. Comparison of the frequency of the Γ-point optical phonon and third-order force constant k_{xyz} in Si calculated from total-energy and atomic forces, results of LAPW, pseudopotential, and FP-LMTO calculations as well as the experiment.

	ω (THz)	k_{xyz} (Ry/a_B^3)
Present work:		
Total energy	15.43	0.4304
Atomic force	15.51	0.4338
LAPW:[a]		
Total energy	15.37	0.4026
Atomic force	15.40	0.4030
Pseudopotential:[b]		
Total energy	15.16	0.357
Atomic force	15.14	0.355
FP-LMTO:[c]		
Total energy	15.47	0.4212
Experiment	15.53[d]	0.3820[e]

[a]Reference 22.
[b]Reference 25.
[c]Reference 16.
[d]Reference 28.
[e]Reference 29.

exactly equal to zero [see formula (45)] as a result of the application of the Hellman-Feynman theorem to the deep core states. This can be also seen from Tables I and II. The derivative of $\delta E_{\rm el}-\delta^s\rho V_C$ gives the contribution connected with the change in electrostatic energy [the second and third terms in (56) which are both referred to hereafter as the electrostatic contribution to the atomic force, $F_{\rm el}$] and the derivative of $\delta E_{\rm xc}-\delta^s\rho V_{\rm xc}$ gives the exchange-correlation contribution to the atomic force, $F_{\rm xc}$, which is the fourth term in (56). [We also call the last term in (56) a MT-zero contribution to the force, F_0.] The numerically derived forces are presented in Table III where they are compared with the forces calculated after formula (56) using charge densities, potentials, and wave functions obtained for the $y=0$ atomic geometry. Calculated forces in the table are given at the Si atom and at the empty site while the total calculated force is taken as their superposition. We see that the agreement between calculated and numerical values for $F_{\rm el}$, $F_{\rm xc}$, and F_0 is excellent and the discrepancy in the total atomic force is connected with the approximate evaluation of the band contribution $F_{\rm bnd}$. The calculated value of $F_{\rm bnd}$ is 2.7% smaller than estimated numerically which is explained by neglecting the variations $\delta^s\phi,\delta^s\dot{\phi}$ in the derivation of formula (54). Since, on the other hand, the band contribution consists of only 26% from $F_{\rm tot}$ the disagreement between total calculated and numerical forces is only 0.8%. From Table III we also see that the artificial forces at the empty sites are one to two orders of magnitude smaller than the corresponding Si forces and are comparable with the error in determination of $F_{\rm bnd}$. The total force at the empty site is only 1.4% from the total Si force which can obviously be neglected.

After numerical testing of the formulas for atomic forces we compute the frequency of a zone-center optical phonon in Si. We use a dense mesh for BZ integration (150 **k** points) and the results of our calculations are presented in Table IV. There we give the values of the frequency for this mode and third-order force constant k_{xyz} obtained both from total-energy and force calculations. The results are also compared with the LAPW calculations of Yu, Singh, and Krakauer,[22] pseudopotential calculations of Yin and Cohen,[25] another full-potential LMTO calculation of Methfessel, Rodriguez, and Andersen[16] as well as with the experiment. We again see that the agreement between total-energy and force calculations is excellent. The discrepancy is comparable with that of LAPW and pseudopotential calculations and is about 0.5%. All the results are in good agreement with experiment and the accuracy of the present calculation is close to that of another FP-LMTO calculation as well as the results of Yu, Singh, and Krakauer and Yin and Cohen.

Total energies and forces are computed for a zone-boundary H phonon in Nb. The longitudinal and transverse modes of the bcc structure at the H point $(001)2\pi/a$ are degenerate. ($a=6.22$ a.u. is the experimental lattice parameter.) The details of the calculations are as follows. We use 1κ-s,p,d-basis set having the one-center spherical harmonics expansion truncated at $l_{\rm max}=8$. The fixed tail energy is chosen to be 0.5 Ry approximately at the center of the occupied part of the band with a small imaginary part 0.03 Ry. $4s$ and $4p$ states are also treated as valence states with the tail energies -3 and -1.5 Ry, respectively. The MT radius of Nb is chosen to be 2.568 a.u. and 60 **k** points are used for BZ integration by means of the tetrahedron method. Table V presents calculated total energy for four distorted configurations with respect to the equilibrium geometry. The displacements δ are given for a single atom in units of lattice parameter. To derive numerically the atomic forces we use a sixth-order even-powered (due to symmetry) polynomial interpolation and determine the force at each value δ. The numerical forces are given in Table V where they are compared with those calculated after formula (56).[26] We see that the discrepancy between them is less than 1.8% which is close to the discrepancy 0.8% found earlier for Si. Using this data analysis we estimate the frequency of the H pho-

TABLE V. Calculated total energy with respect to the equilibrium configuration as a function of distortion (in units of a) for the H-point phonon in Nb. Comparison between numerically derived ($F_{\rm num}$) and calculated ($F_{\rm calc}$) forces.

δ	0.005	0.010	0.015	0.020
$\Delta E_{\rm tot}$ (mRy)	0.166 8	0.678 1	1.569 6	2.840 3
$F_{\rm num}$ (Ry/a_B)	0.010 73	0.022 41	0.034 94	0.046 23
$F_{\rm calc}$ (Ry/a_B)	0.010 70	0.022 33	0.034 53	0.047 06

TABLE VI. Comparison of calculations from the total energy and atomic forces as well as measured frequencies for the X-point phonon in Al. The values are given in THz.

	Total energy	Atomic force	Experiment[a]
Longitudinal	9.38	10.05	9.69
Transverse	5.62	6.07	5.79

[a]Reference 27.

non which is found from the total-energy calculations to be 6.56 THz. The results of force calculations give the value 6.60 THz which is only 0.7% larger than the previous one and is 1.7% larger than the experimental frequency of 6.49 THz.[27] We thus conclude that the agreement with experiment is good.

As a final example let us consider the calculation concerning a zone-boundary X phonon in fcc Al. We use $3s$, $3p$, and $3d$ muffin-tin orbitals for representing valence states with the tail energy $\kappa^2=0.3$ Ry. ($\mathrm{Im}\kappa^2$ is set to 0.03 Ry just as in the previous calculations.) $2s$ and $2p$ MT orbitals are used for higher-lying core states with κ^2 equal to -6.5 and -4 Ry, respectively. All the basis has the one-center spherical harmonics expansion up to $l_{\max}=6$. The lattice constant a is taken as 7.64 a.u. and the MT radius of Al is chosen to be 2.623 a.u. Since in the fcc structure at the point $X=(001)2\pi/a$ longitudinal and transverse modes are nondegenerate we perform two separate calculations. For the longitudinal mode 75 **k** points are used for taking BZ integrals while for the lower symmetry transverse mode 150 **k** points are employed. The results are presented in Table VI where they are compared with the measured phonon frequencies.[27] The agreement between total-energy and force calculations is good but the discrepancy is larger than found for Si and Nb and is about 7%. All theoretical values are very close to the experiment with the accuracy better than 4.5%.

VII. CONCLUSION

In conclusion, we have presented an efficient approach for inclusion of full-potential terms in the LMTO method. By using the partition of crystalline space on the atom-centered cell envelopes and one-center spherical harmonics expansions all the integrals over the interstitial region are evaluated accurately. It was shown how they can be expressed through the constants depending only on the crystalline structure and calculated explicitly. This led to a fast and uncomplicated full-potential scheme which can be inserted rapidly into existing computer programs. The method was applied to the frozen-phonon calculations and the formulation for atomic forces has been given. The force is represented as a direct variation of every contribution to the total energy in the LMTO framework which can be tested easily in terms of the usual total-energy analysis. The total-energy and force calculations for phonon frequencies in various systems have been presented which are found to be in good agreement with the results of previous calculations as well as with the experiment.

ACKNOWLEDGMENTS

The authors are indebted to Professor O. K. Anderson for many helpful discussions. One of us (S.Y.S.) would like to acknowledge the support of the Max-Planck-Gesellschaft.

APPENDIX: DETAILS ON VARIATION IN EIGENVALUES

The task is to calculate the change in the eigenvalue $\varepsilon_{\mathbf{k}\lambda}$ as given by formula (53). We first derive the change in the Hamiltonian matrix by assuming that MT orbitals $\chi^{\mathbf{k}}_{\kappa R+\delta RL}$ in the final atomic configuration are constructed in terms of $\phi_{\kappa RL}$ and $\dot{\phi}_{\kappa RL}$ found for the original crystal. We write

$$\delta H^{\mathbf{k}}_{\kappa' R'L'\kappa RL}=H^{\mathbf{k}}_{\kappa' R'+\delta R'L'\kappa R+\delta RL}-H^{\mathbf{k}}_{\kappa' R'L'\kappa RL}$$
$$=\sum_{R_0}\langle\chi^{\mathbf{k}}_{\kappa' R'+\delta R'L'}|-\nabla^2+\tilde{V}_{R_0+\delta R_0}|\chi^{\mathbf{k}}_{\kappa R+\delta RL}\rangle_{\Omega_{R_0}}-\sum_{R_0}\langle\chi^{\mathbf{k}}_{\kappa' R'L'}|-\nabla^2+V_{R_0}|\chi^{\mathbf{k}}_{\kappa RL}\rangle_{\Omega_{R_0}}\,, \tag{A1}$$

where the potential $\tilde{V}_{R+\delta R}$ is the exact potential for the final configuration centered at sites $R+\delta R$ while the polyhedron partition Ω_R for both geometries is supposed to be the same. We now divide the integration into the MT and interstitial regions, introduce the potential $V_{R+\delta R}$ of the original lattice centered at sites $R+\delta R$ and continue:

$$\delta H^{\mathbf{k}}_{\kappa' R'L'\kappa RL}=\sum_{R_0}\langle\chi^{\mathbf{k}}_{\kappa' R'+\delta R'L'}|-\nabla^2+V_{R_0+\delta R_0}|\chi^{\mathbf{k}}_{\kappa R+\delta RL}\rangle_{s_{R_0}}-\sum_{R_0}\langle\chi^{\mathbf{k}}_{\kappa' R'L'}|-\nabla^2+V_{R_0}|\chi^{\mathbf{k}}_{\kappa RL}\rangle_{s_{R_0}}$$
$$+\kappa^2\langle\chi^{\mathbf{k}}_{\kappa' R'+\delta R'L'}|\chi^{\mathbf{k}}_{\kappa R+\delta RL}\rangle_{\tilde{\Omega}^{\mathrm{int}}}-\kappa^2\langle\chi^{\mathbf{k}}_{\kappa' R'L'}|\chi^{\mathbf{k}}_{\kappa RL}\rangle_{\Omega^{\mathrm{int}}}\sum_{R_0}\langle\chi^{\mathbf{k}}_{\kappa' R'+\delta R'L'}|V_{R_0+\delta R_0}|\chi^{\mathbf{k}}_{\kappa R+\delta RL}\rangle_{\tilde{\Omega}^{\mathrm{int}}_{R_0}}$$
$$-\sum_{R_0}\langle\chi^{\mathbf{k}}_{\kappa' R'L'}|V_{R_0}|\chi^{\mathbf{k}}_{\kappa RL}\rangle_{\Omega^{\mathrm{int}}_{R_0}}+\sum_{R_0}\langle\chi^{\mathbf{k}}_{\kappa' R'L'}|\delta^s V_{R_0}|\chi^{\mathbf{k}}_{\kappa RL}\rangle_{\Omega_{R_0}}\,, \tag{A2}$$

where the kinetic energy matrix elements are taken over interstitial regions $\tilde{\Omega}^{\mathrm{int}}$, Ω^{int} without partition on the polyhedra (see text), where $\tilde{\Omega}_R{}^{\mathrm{int}}$ stands for the interstitial region: $\Omega_R-s_{R+\delta R}$ defined with shifted MT sphere while Ω^{int}_R is Ω_R-s_R and where $\delta^s V_R=\tilde{V}_R-V_R$ is the soft variation in the effective potential. We see that the difference between first and second terms and between the third and fourth terms in (A2) is expressed via the change in the structure con-

stants. This is because all radial matrix elements in the MT part of the Hamiltonian are defined with the same potential, radial functions centered at the corresponding MT spheres. The radial matrix elements for the kinetic energy in the interstitial region are just Wronskians [see (12), (13)] and depend only on the MT-sphere radii but not on their positions.

Some care should be taken to calculate the difference between the interstitial-potential matrix elements [fifth and sixth terms in (A2)]. Since they are calculated using one-center expansions for LMTO's we now redefine the interstitial volumes for the final atomic configuration to make the radial matrix elements in both geometries coincide. This is done by shifting the whole polyhedron Ω_R together with its nucleus (not only the MT sphere as assumed before). We introduce $\Omega^{\rm int}_{R+\delta R}$ which is $\Omega_{R+\delta R}-s_{R+\delta R}$. With this definition the difference between fifth and sixth contribution in (A2) is expressed via the change in the structure constants plus the integral over the surfaces of the polyhedra. We arrive at

$$\delta H^{\mathbf{k}}_{\kappa' R' L' \kappa R L}=\sum_{R_0}\delta\mathbf{R}_0\frac{d}{d\mathbf{R}_0}H^{\mathbf{k}}_{\kappa' R' L' \kappa R L}+\sum_{R_0}\delta R_0\langle\chi^{\mathbf{k}}_{\kappa' R' L'}|V_{R_0}|\chi^{\mathbf{k}}_{\kappa R L}\rangle_{S^{\rm pol}_{R_0}}+\sum_{R_0}\langle\chi^{\mathbf{k}}_{\kappa' R' L'}|\delta^s V_{R_0}|\chi^{\mathbf{k}}_{\kappa R L}\rangle_{\Omega_{R_0}}, \tag{A3}$$

where the derivative $d/d\mathbf{R}$ here means that only structure constants have to be differentiated and where the second term is the integral over the surface $S^{\rm pol}_R$ of the polyhedron. The latter can be represented as the volume integral taken with the gradient of the integrand function which gives

$$\delta H^{\mathbf{k}}_{\kappa' R' L' \kappa R L}=\sum_{R_0}\delta\mathbf{R}_0\frac{d}{d\mathbf{R}_0}H^{\mathbf{k}}_{\kappa' R' L' \kappa R L}+\sum_{R_0}\delta\mathbf{R}_0\int_{\Omega_{R_0}}V_{R_0}(\mathbf{r}_{R_0})\nabla[\chi^{\mathbf{k}*}_{\kappa' R' L'}(\mathbf{r}_{R_0})\chi^{\mathbf{k}}_{\kappa R L}(r_{R_0})]d\mathbf{r}_{R_0}+\sum_{R_0}\langle\chi^{\mathbf{k}}_{\kappa' R' L'}|\delta V_{R_0}|\chi^{\mathbf{k}}_{\kappa R L}\rangle_{\Omega_{R_0}}, \tag{A4}$$

where δV_{R_0} is the full change in the potential.

The variation in the overlap matrix is calculated analogously. Since we do not use one-center expansions for LMTO's to calculate interstitial overlap integrals we just obtain

$$\delta O^{\mathbf{k}}_{\kappa' R' L' \kappa R L}=\sum_{R_0}\delta R_0\frac{d}{d\mathbf{R}_0}O^{\mathbf{k}}_{\kappa' R' L' \kappa R L}, \tag{A5}$$

expressing it via the change in the structure constants. By multiplying (A4) and (A5) by $A^{\mathbf{k}\lambda *}_{\kappa' R' L'}$, $A^{\mathbf{k}\lambda}_{\kappa' R' L'}$, and summing over $\kappa' R' L'$, $\kappa R L$ we come to formula (54).

*On leave from P. N. Lebedev Physical Institute of the Russian Academy of Sciences, Moscow, Russia.

[1]P. Hohenberg and W. Kohn, Phys. Rev. **136**, B864 (1964); W. Kohn and L. J. Sham, *ibid.* **140**, A1133 (1965); for a review see also *Theory of the Inhomogeneous Electron Gas*, edited by S. Lundqvist and N. H. March (Plenum, New York, 1983).

[2]See, e.g., *Ab Initio Calculations of Phonon Spectra*, edited by J. T. Devreese, V. E. Van Doren, and P. E. Van Camp (Plenum, New York, 1983).

[3]A. Fleszar and R. Resta, Phys. Rev. B **31**, 5305 (1985); K. Kunc and E. Tosatti, *ibid.* **29**, 7045 (1985).

[4]B. Drittler, M. Weinert, R. Zeller, and P. H. Dederics, Solid State Commun. **79**, 31 (1991); P. H. Dederichs, T. Hoshino, B. Drittler, K. Abraham, and R. Zeller, Physica B **172**, 203 (1991).

[5]H. Wendel and R. M. Martin, Phys. Rev. B **19**, 5251 (1979).

[6]O. K. Andersen, Phys. Rev. B **12**, 3060 (1975).

[7]O. K. Andersen and R. G. Wooley, Mol. Phys. **26**, 905 (1973).

[8]D. D. Koelling and G. O. Arbman, J. Phys. F **5**, 2041 (1975).

[9]K. H. Weyrich, Phys. Rev. B **37**, 10 269 (1988).

[10]P. Blöchl, Ph.D. thesis, Max-Planck-Institut für Festkörperforschung, 1989.

[11]M. Methfessel, Phys. Rev. B **38**, 1537 (1988).

[12]P. Pulay, Mol. Phys. **17**, 197 (1969).

[13]D. Glötzel, B. Segall, and O. K. Andersen, Solid State Commun. **36**, 403 (1980).

[14]See, e.g., O. K. Andersen, in *Electronic Structure of Complex Systems*, edited by P. Phariseaux and W. Temmerman (Reidel, Dordrecht, 1984); F. Casula and F. Herman, J. Chem. Phys. **78**, 858 (1983); M. Sprinborg and O. K. Andersen, *ibid.* **87**, 7125 (1987).

[15]M. Sprinborg and O. K. Andersen, Ref. 14.

[16]M. Methfessel, C. O. Rodriguez, and O. K. Andersen, Phys. Rev. B **40**, 2009 (1989).

[17]See, e.g., O. K. Andersen, O. Jepsen, and M. Sob, in *Electronic Band Structure and its Applications*, edited by M. Yussouff, Lecture Notes in Physics Vol. 283 (Springer, Berlin, 1987); A. M. Bratkovsky and S. Yu. Savrasov, J. Comput. Phys. **88**, 243 (1990).

[18]*Handbook of Mathematical Functions*, edited by M. Abramowitz and I. A. Stegun (Dover, New York, 1964).

[19]J. Molenaar, J. Phys. C **21**, 1455 (1988); A. Gonis, X.-G. Zhang, and D. M. Nicholson, Phys. Rev. B **38**, 3564 (1988); R. Zeller, *ibid.* **38**, 5993 (1988).

[20]J. Harris, R. O. Jones, and J. E. Muller, J. Chem. Phys. **75**, 3904 (1981); P. Blöchl, Ref. 10; L. M. Soler and A. R. Williams, Phys. Rev. B **40**, 1560 (1989).

[21]A. R. Mackintosh and O. K. Andersen, in *Electrons at the Fermi Surface*, edited by M. Springford (Cambridge University Press, England, 1990), p. 149.

[22]R. Yu, D. Singh, and H. Krakauer, Phys. Rev. B **43**, 6411 (1991).

[23]V. L. Moruzzi, J. F. Janak, and A. R. Williams, *Calculated Electronic Properties of Metals* (Pergamon, New York, 1978).

[24]O. Jepsen and O. K. Andersen, Solid State Commun. **8**, 1763 (1971).

[25]M. T. Yin and M. L. Cohen, Phys. Rev. B **26**, 3259 (1982).

[26]Via the use of the tetrahedron method with finite sampling for

metals some small residual value for the atomic force at the equilibrium configuration is retained. This residual force is found by extrapolation from the calculations for distorted geometries and the forces presented in Table V have been corrected on this value.

[27]*Numerical Data and Functional Relationships in Science and Technology*, Landolt-Börnstein, New Series, Vol. 13, Pt. a (Springer, Berlin, 1981).

[28]*Numerical Data and Functional Relationships in Science and Technology*, Landolt-Börnstein, New Series, Vol. 22, Pt. a (Springer, Berlin, 1982).

[29]H. J. McSkimin and P. Andreatch, J. Appl. Phys. **35**, 3312 (1965).